05

Effect of low-cycle fatigue on acoustic birefringence in austenitic steel AISI 321

© V.A. Klyushnikov, A.V. Gonchar

Federal Research Center A.V. Gaponov-Grekhov Institute of Applied Physics of the Russian Academy of Sciences,
603024 Nizhny Novgorod, Russia
e-mail:ndt@ipmran.ru

Received June 20, 2023
Revised November 10, 2023
Accepted November 16, 2023

This paper presents the results of a study of the effect of low-cycle fatigue on acoustic birefringence in austenitic stainless steel AISI 321 at test temperature 20 and 60°C. A model was proposed, which represents acoustic birefringence of entire material as the sum of two separate components for soft matrix of austenite and hard inclusions of α'-martensite. Changes in acoustic birefringence caused by deformation of austenite and martensitic transformation under fatigue were compared using calculations based on the data obtained earlier for uniaxial tension of the same steel. The kinetics of changes in acoustic birefringence of austenite was analyzed with and without taking into account the effect of martensitic transformation. The results have practical importance for the development of ultrasonic techniques for nondestructive evaluation of the state of metastable austenitic steel.

Keywords: austenitic stainless steel, test temperature, deformation-induced martensitic transformation, ultrasonic method, acoustic birefringence, eddy current method.

DOI: 10.61011/JTF.2024.01.56901.152-23

Introduction

Austenitic stainless steel is widely used in the creation of structures for nuclear, chemical and other industries. It is known that plastic deformation of most steels of this class with low energy of stacking faults, even at room temperature, simultaneously with the accumulation of damage is accompanied by a phase transformation of austenite into strain-induced α'-martensite [1,2]. The intensity of the strain-induced martensitic transformation depends on external factors such as the loading frequency [3–5] and the temperature [6–8].

The difference between the elasticity modules α'-martensite and austenite results in a change of the modulus of elasticity and acoustic parameters of the entire volume of the material. The formation of α'-martensite also affects the viscosity and hardness of steel [9–11] and results in a change of the intensity of damage accumulation [12]. Previous work showed that the intensity of strain-induced transformation of martensite decreases down to zero with the increase of temperature under loading [6,13,14]. At the same time, damage accumulates in the material, which is practically not studied.

There are many studies devoted to the study of changes in properties during loading of austenitic steels by magnetic or eddy current control methods [15–19]. However, studies of changes of the acoustic [19–21] or electrical properties [22,23] are interest with respect to determination of the damage.

The impact of static loading and fatigue on the anisotropy of the elastic properties of steel AISI 321 at different test temperatures was studied in this paper. The anisotropy of elastic properties was described using the acoustic birefringence parameter B which is defined as:

$$B = 2\frac{t_x - t_y}{t_x + t_y}, \tag{1}$$

where the propagation time of two shear waves propagating between two plane-parallel areas of specimen and polarized in a mutually perpendicular direction, along loading axis t_x and across loading axis t_y.

The birefringence parameter in the entire material was presented based on experimental data as the sum of two components for a soft matrix of austenite and solid inclusions of strain-induced α'-martensite.

1. Experimental procedure

Austenitic stainless steel AISI 321 was studied in this paper, the chemical composition is provided in the table.

The shapes and sizes of the specimen are shown in Fig. 1. Plane-parallel pads were cut on both sides of the working area on each specimen for ultrasonic and eddy current measurements.

The mechanical step-by-step tests were conducted using servo-hydraulic testing system BISS Nano UT-01-0025. Ultrasonic and eddy current measurements were performed before the test and after each loading stage. Thermocouples were attached to the center of the sample and the lower and upper jaws of the testing system to measure the temperature.

The static loading was performed at a strain rate of $5 \cdot 10^{-3}\,s^{-1}$ at temperatures of 20, 40 and 60°C.

Chemical composition of the studied steel AISI 321 (%)

C	Cr	Ni	Mn	Mo	Ti	P	S	Si	Fe
0.03	17.27	9.02	0.56	0.22	0.31	0.029	0.003	0.43	Base

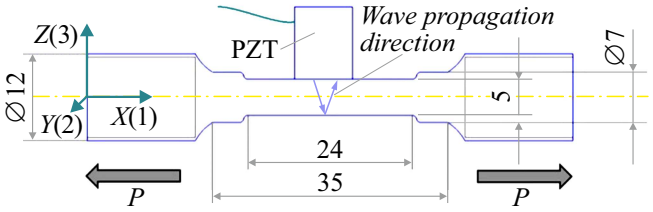

Figure 1. Acoustic measurement scheme; $X(1)$, $Y(2)$ and $Z(3)$ — the axes of symmetry of the specimen.

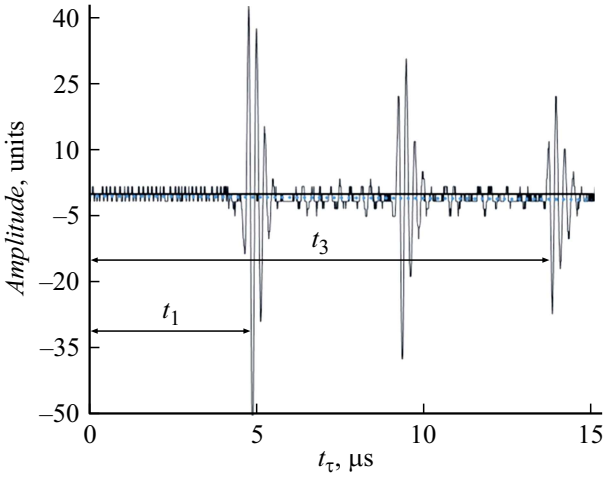

Figure 2. Amplitude-time diagram of shear waves.

Low-cycle fatigue tests were carried out by monitoring the complete strain of the cycle with an asymmetry coefficient $R_\varepsilon = 0$ and a constant strain rate $5 \cdot 10^{-3}\,\mathrm{s}^{-1}$. Uniaxial cyclic loading P is directed along the axis $X(1)$ (Fig. 1). The total strain amplitude $\Delta\varepsilon/2$ was 0.3 and 0.5%, temperature was 20 and 60°s. The tests were stopped when the stresses in the cycle dropped by 50% compared to the steady-state stress value in accordance with GOST 25.505-85.

The amplitude-time diagrams of echo pulses were recorded for measuring the ultrasonic wave propagation time t_x and t_y (Fig. 2). The ultrasonic wave propagation time t_τ was measured between the first signal t_1 and the third signal t_3. The S- wave was excited and received by a wide-band piezoelectric transducer (PET) V157 Olympus having element 3.2 mm in size with center frequency of 5 MHz. The commercially available ultrasonic flaw detector A1212 MASTER was used as an electrical pulse generator. Amplitude-time diagrams of signals from the PET were recorded on a personal computer using LA-n1USB digital oscilloscope and ADCLab software. The maximum sampling rate of the oscilloscope is 1 GHz, time resolution is 1 ns.

A multifunctional eddy current device MVP-2M with a frequency sensor 1 kHz was used for measuring eddy current. It was originally developed to measure the ferrite content in austenitic and pearlite grade steels. The device was calibrated by the manufacturer. The obtained results of measuring the content of α'-martensite were indicated in percentages of ferrite like in [10] since the magnetic properties of ferrite and ferromagnetic α'-martensite differ slightly [24].

2. Results of investigation

2.1. Cyclic hardening and softening

An increase of the voltage amplitude (cyclic hardening) is observed regardless of the test temperature at the strain amplitude of 0.5% (Fig. 3). Cyclic hardening is caused by several factors: an increase of the number of stacking faults [25], an increase of the density of dislocations in austenite [26], as well as the formation of strain-induced α'-martensite. Softening is observed after initial hardening at 0.3% strain amplitude. Cyclic softening occurs when the rate of dislocation annihilation exceeds the rate of their generation, causing a general decrease of dislocation density, or when dislocations are rearranged into a cellular structure, which results in an

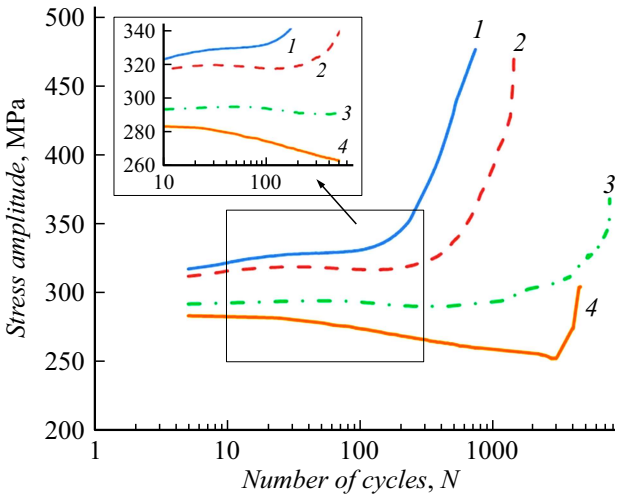

Figure 3. Stress amplitude during cyclic loading at $\Delta\varepsilon/2 = 0.5\%$ and $T = 20°\mathrm{C}$ (*1*), $\Delta\varepsilon/2 = 0.5\%$ $T = 60°\mathrm{C}$ (*2*), $\Delta\varepsilon/2 = 0.3\%$ and $T = 20°\mathrm{C}$ (*3*), $\Delta\varepsilon/2 = 0.3\%$ and $T = 60°\mathrm{C}$ (*4*).

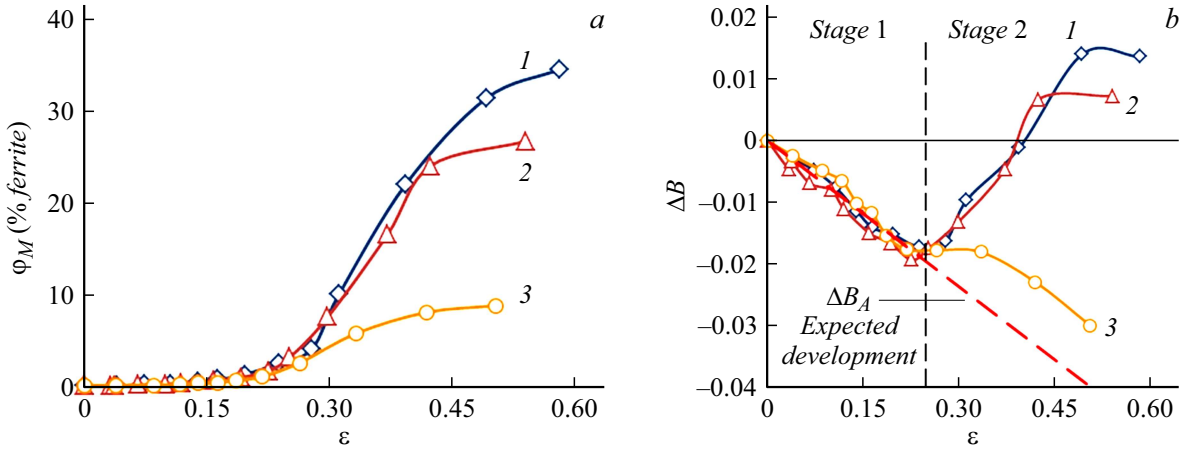

Figure 4. Dependence of the volume fraction of α'-martensite φ_M (a) and ΔB (b) on plastic strain ε for steel AISI 321 at test temperatures: 20 (*1*), 40 (*2*) and 60°C (*3*) [24].

increase of the free path of dislocations [27,28]. It is worth noting that the decrease of stress amplitude at temperature of 60°C is more significant than at temperature of 20°C.

The active formation of α'-martensite starts after a certain number of cycles which depends on the loading conditions which counteracts a decrease of the density of dislocations of austenite [29] and results in the secondary hardening up to the destruction of the sample.

2.2. Results of acoustic and eddy current measurements under static tension

A clear dependence of the kinetics of α'-martensite on the test temperature is observed at static tension (Fig. 4, a). The experimental data (Fig. 4, b) are consistent with the theoretical calculations of [30]. The authors showed that the acoustic birefringence B decreases with static loading of a material with a FCC lattice and increases with deformation of a material with a BCC lattice. Fig. 4, b shows that austenite with a FCC lattice prevails in the material at stage 1 (parameter B decreases). An intensive martensitic transformation begins at stage 2 (Fig. 4, b), which affects the kinetics of change of parameter B. The obtained dependences reflect the cumulative effect of damage accumulation, texture changes in austenite with a FCC lattice and the formation of strain-induced α'-martensite with a BCC lattice at different static loading temperatures of stainless steel AISI 321.

2.3. Results of acoustic and eddy current measurements at fatigue

An intensive increase of the volume fraction φ_M of strain-induced α'-martensite is observed in all loading conditions after the relative number of loading cycles $N/N_f = 0.2$ (N_f — the number of cycles before the formation of a macroscopic crack) (Fig. 5, a). Fig. 3 and 5, a show that the hardening of the material under cyclic loading corresponds very well to the kinetics of martensitic transformation. As a matter of fact, cyclic hardening of austenitic steel occurs due to the martensitic transformation [32]. It is expected that the strain-induced α'-martensite volume fraction φ_M for both strain amplitudes after testing at temperature 60°C is less than at 20°C. It should be noted that the dependence $\sqrt{\varphi_M}$ on the number of cycles N can be approximated by a linear function, and the angle of inclination reflects the magnitude of the strain amplitude and the loading temperature (insert in Fig. 5, a).

The change of B under fatigue of B was obtained in all loading conditions from ultrasonic studies (Fig. 5, b). It should be noted that B increases at the initial stages of loading with a strain amplitude of 0.3% and decreases with further loading. The birefringence parameter decreases at all loading stages at both temperatures at 0.5% strain amplitude and the nature of the change of B for the studied temperatures coincides. A difference of the nature of the change of B is observed with further loading, which is determined by the different rate of formation of the α'-martensite phase. Therefore an increase of the deformation temperature contributes to an increase of B with the same strain amplitude. The variation of B with a strain amplitude of 0.5% is similar to the variation under static loading, since the curves merge at the first stages of loading and then they diverge.

Accordingly, B increases with the strain amplitude of 0.3% in the early stages and it can be concluded that the rate of formation of martensite is so small that it does not significantly affect the elasticity constants of austenite with a FCC lattice. α'-martensite with a BCC lattice begins to form more intensively when the relative number of loading cycles reaches 0.2, which results in a decrease of B. Thus, the kinetics of the change of B reflects the nature of hardening and softening at the studied strain amplitude and temperatures.

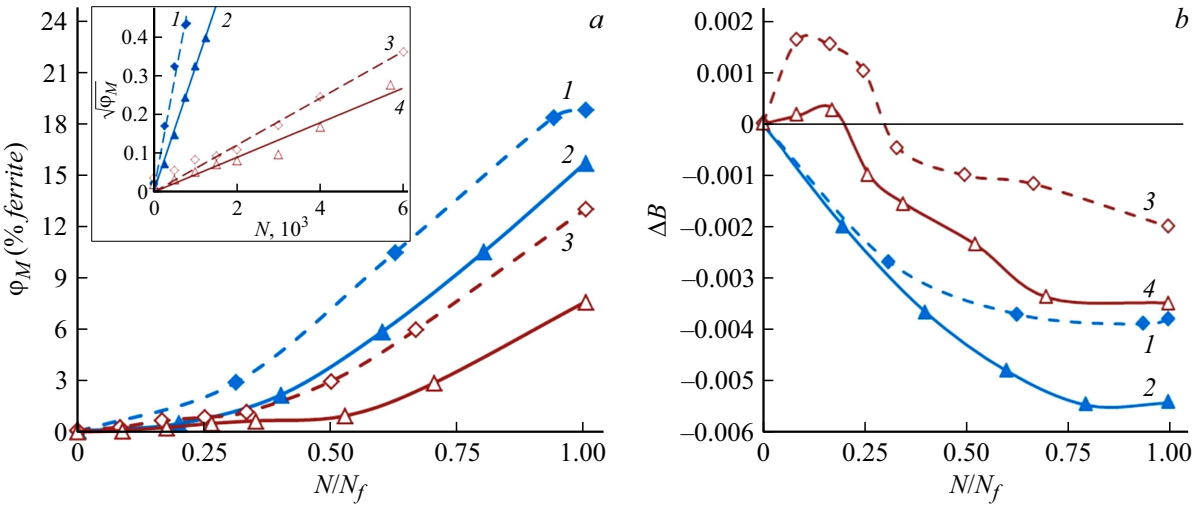

Figure 5. Change of φ_M (a) and B (b) under cyclic loading at $\Delta\varepsilon/2 = 0.5\%$ and $T = 20°C$ (*1*), $\Delta\varepsilon/2 = 0.5\%$ and $T = 60°C$ (*2*), $\Delta\varepsilon/2 = 0.3\%$ and $T = 20°C$ (*3*), $\Delta\varepsilon/2 = 0.3\%$ and $T = 60°C$ (*4*).

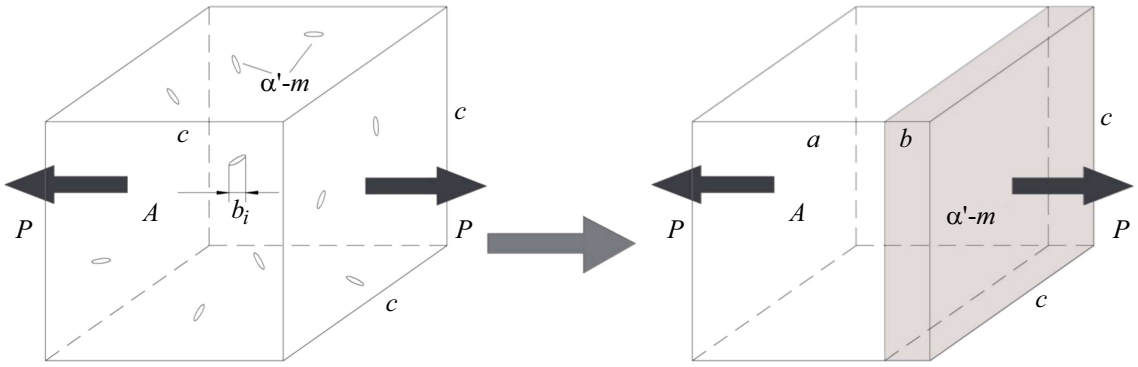

Figure 6. Representative volume of the austenite matrix with inclusions of α'-martensite.

3. Discussion

Let's calculate the change of the birefringence parameter $B_{A\text{eff}}$ taking into account the martensitic transformation during static loading. Let's consider for this purpose a representative element of cubic volume with an edge of length c, which is affected by a load P (Fig. 6). It contains a certain volume fraction of strain-induced α'-martensite φ_M. The following assumptions will be used for the calculation:

— The two-phase material consists of a soft austenitic matrix and solid martensitic inclusions randomly distributed in the matrix;

— α'-martensite does not deform;

— The formation of martensite has no effect on the deformation of austenite.

Let the effective size of each inclusion be b_i, and the entire martensite phase occupies the volume c^2b, where $b = \sum_i b_i$.

Then the volume fraction of the α'-martensite is $\varphi_M = \frac{c^2 b}{c^3} = \frac{b}{c}$, the volume fraction of the austenite phase is $\varphi_A = 1 - \varphi_M = \frac{a}{c}$.

The strain ε_S measured by the extensometer during testing can be recorded via a, b and c:

$$\varepsilon_S = \frac{\Delta c}{c} = \frac{\Delta a}{a+b}. \tag{2}$$

Then the strain of austenite ε_A can be determined using the following formula:

$$\varepsilon_A = \frac{\Delta a}{a}. \tag{3}$$

The strain ratio is written as

$$\frac{\varepsilon_A}{\varepsilon_S} = \frac{1}{1-\varphi_M}. \tag{4}$$

In formulas, the volume fraction of α'-martensite is given in fractions, it is shown as a percentage in figures, except for the insert in Fig. 5, *a*.

The change in ΔB is attributable not only to the accumulation of damage [21] and a change of texture, but also to the formation of α'-martensite. We write down the change of ΔB of the entire material in the following

form assuming that under static loading, the kinetics of the change of the birefringence parameter in austenite remains constant even with the formation of α'-martensite, and the birefringence parameter in the resulting martensite depends only on its volume fraction

$$\Delta B = \Delta B_A + \Delta B_M, \tag{5}$$

where ΔB_A — determines the change of the birefringence parameter in austenite because of its deformation, ΔB_M — determines the change of the birefringence parameter because of the formation of α'-martensite.

The change of ΔB_1 for the entire material can be approximated by a linear dependence on plastic strain ε at the first stage of static loading (stage 1, Fig. 4, *b*) with an insignificant intensity of martensitic transformation:

$$\Delta B_1 = \Delta B_A = -0.086\varepsilon. \tag{6}$$

The change of the birefringence parameter $B_{A\text{eff}}$ (Fig. 4, *b*), taking into account equations (2), (3) and (6), can be expressed as follows:

$$B_{A\text{eff}} = -\frac{0.086\varepsilon}{1-\varphi_M}. \tag{7}$$

The change of the birefringence parameter $B_{M\text{eff}}$ will be defined as:

$$\Delta B_{M\text{eff}} = \Delta B + \frac{0.086\varepsilon}{1-\varphi_M}. \tag{8}$$

During the plastic loading the proportion of α'-martensite increases and plastic strain concentrates in softer austenite, which results in an increase of the intensity of the change of the birefringence parameter $B_{A\text{eff}}$.

A decrease of the intensity of martensitic transformation has a greater effect on $B_{M\text{eff}}$ than on $B_{A\text{eff}}$ (Fig. 7). For instance, $\Delta B_{M\text{eff}}$ in case of failure at temperature of 20°C is approximately 8 times greater, than at temperature of 60°C, $\Delta B_{A\text{eff}}$ is greater by about 1.5 times.

It was found that the change of the birefringence parameter B_M at the 2nd stage of static loading in the temperature range from 20 to 60°C linearly depends on the percentage of α'-martensite φ_M (Fig. 8):

$$\Delta B_M = 0.17\varphi_M. \tag{9}$$

We determine the change B_A in austenite under fatigue using equations (5) and (9) based on the assumption that the parameter B_M changes due to fatigue in the same way as under static loading:

$$\Delta B_A = \Delta B - 0.17\varphi_M. \tag{10}$$

The value of ΔB_A shows a change of the birefringence parameter in austenite without taking into account the intensity of formation of α'-martensite. Fig. 5, *b* and 9 *a* show that ΔB_A is significantly larger than ΔB and exceeds the latter by about 7–10 times when destroyed, i.e., the martensitic transformation due to fatigue also contributes to

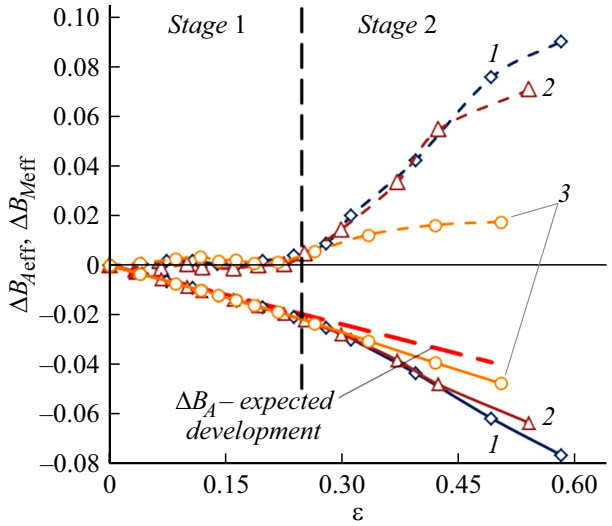

Figure 7. Dependence of the change $B_{A\text{eff}}$ (solid line) and $B_{M\text{eff}}$ (dashed line) on the strain ε at $T = 20$ (*1*), 40 (*2*) and 60°C (*3*).

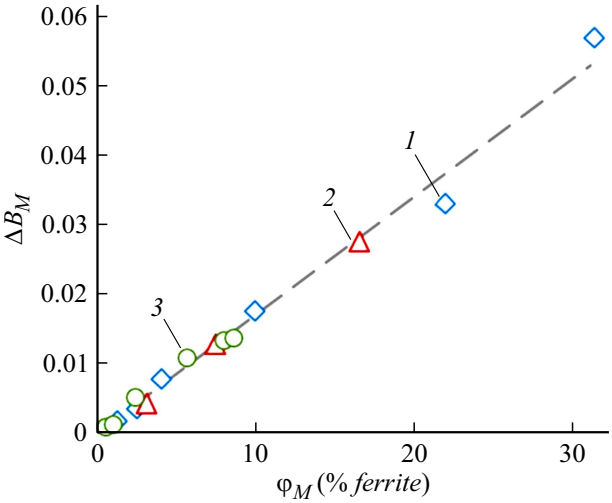

Figure 8. The relationship of B_M and the volume fraction of α'-martensite at the 2nd stage of static loading of steel AISI 321 at $T = 20$ (*1*), 40 (*2*) and 60°C (*3*) [24].

an increase of ΔB, which corresponds to Fig. 4, *b*, which indicates the expected development of B (dashed line) without phase transformations.

We obtain a change of the birefringence parameter in austenite $\Delta B_{A\text{eff}}$ under fatigue, the change of which will not depend on the loading conditions, as follows:

$$\Delta B_{A\text{eff}} = 36\sqrt[3]{k}(\Delta B - 0.17\varphi_M). \tag{11}$$

where k — the tangent of the angle of inclination of the dependence $\sqrt{\varphi_M}(N)$ (insert in Fig. 5, *a*), which is $5.8 \cdot 10^{-4}$ at strain amplitude $\Delta\varepsilon/2 = 0.5\%$ and $T = 20$°C, at $T = 60$°C $k = 3.2 \cdot 10^{-4}$. At strain amplitude of $\Delta\varepsilon/2 = 0.3\%$ and $T = 20$°C $k = 6.0 \cdot 10^{-5}$, at $T = 60$°C $k = 4.5 \cdot 10^{-5}$. The coefficients in expression (11) were selected in such a way that the dependence $\Delta B_{A\text{eff}}(N/N_f)$

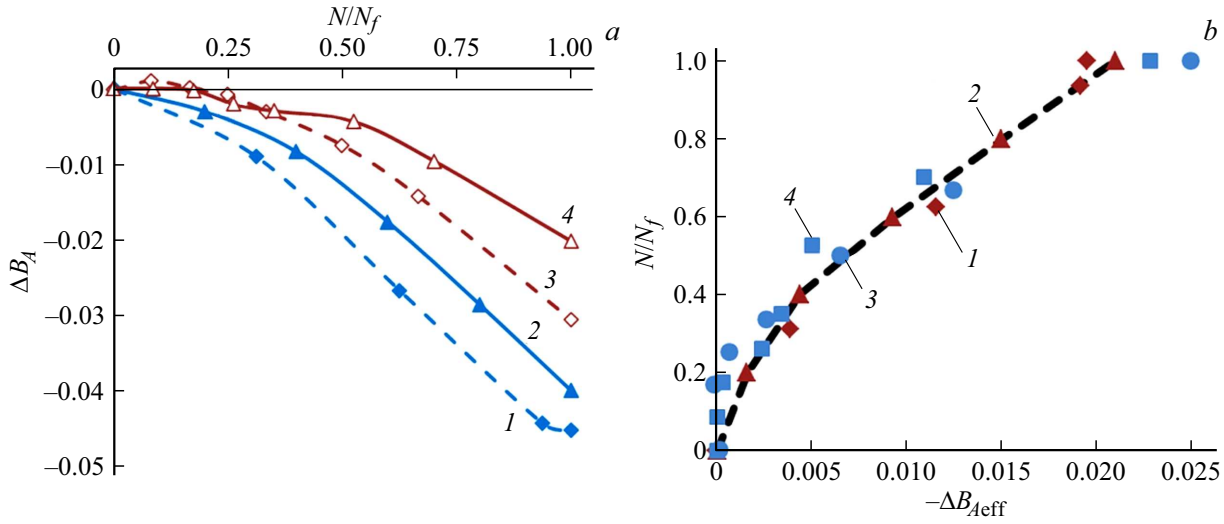

Figure 9. Change of B_A (a) and ΔB_{Aeff} (b) under cyclic loading at $\Delta\varepsilon/2 = 0.5\%$ and $T = 20^\circ$C (*1*), $\Delta\varepsilon/2 = 0.5\%$ and $T = 60^\circ$C (*2*), $\Delta\varepsilon/2 = 0.3\%$ and $T = 20^\circ$C (*3*), $\Delta\varepsilon/2 = 0.3\%$ and $T = 60^\circ$C (*4*).

for all samples was the same at different intensity of phase transformations, due, among other things, to the magnitude of the strain cycle amplitude and temperature.

Fig. 9, *b* shows that the values ΔB_{Aeff} obtained for all loading conditions are superimposed on one curve, and when a crack occurs in the material they reach the value 0.022 ± 0.002. The calculations for stage 2 were made with the assumption that ΔB_{Aeff} changes in the same way as in stage 1.

Therefore, when solving the reverse problem with known values φ_M and B, it is possible to calculate the component ΔB_{Aeff}, which characterizes damage and can be used to assess the current condition of the material.

Conclusion

The kinetics of martensitic transformation affects the mechanical properties and the parameter of acoustic birefringence at fatigue of steel AISI 321.

An increase of softening is observed with an increase of the test temperature which is most pronounced in case of testing with the strain amplitude 0.3%. The relationship between the change of the birefringence parameter B_M and the volume fraction α'-martensite at the second stage of static loading adheres to a linear law in the studied temperature range. The magnitude of the change of the acoustic birefringence parameter during the formation of α'-martensite exceeds the similar change during austenite deformation in accordance with the proposed model. A universal curve of the change of the acoustic birefringence parameter in austenite (when the kinetics of martensitic transformation is slowed down) cause by fatigue was obtained, which describes the results regardless of the loading state and can be used for material diagnostics.

Funding

This study was supported by grant No. 22-29-01237 from the Russian Science Foundation, https://rscf.ru/project/22-29-01237/.

Conflict of interest

The authors declare that they have no conflict of interest.

References

[1] G.B. Olson, M. Cohen. Metall Trans A., **6A**, 791 (1975). DOI: 10.1007/bf02672301
[2] J. Singh. J. Mater. Sci., **20** (9), 3157 (1985). DOI: 10.1007/bf00545181
[3] G. Huang, D. Matlock, G. Krauss. Metall. Trans. A, **20**, 1239 (1989). DOI: 10.1007/BF02647406
[4] J. Talonen, P. Nenonen, G. Pape, H. Hanninen. Metall. Mater. Trans. A, **36A**, 421 (2005). DOI: 10.1007/s11661-006-0220-x
[5] J.A. Lichtenfeld, M.C. Mataya, C.J. van Tyne. Metall. Mater. Trans. A, **37**, 147 (2006). DOI: 10.1007/s11661-006-0160-5
[6] T. Angel. J. Iron Steel Inst., **177**, 165 (1954).
[7] T. Byun, N. Hashimoto, K. Farrell. Acta Mater., **52**, 3889 (2004). DOI: 10.1016/j.actamat.2004.05.003
[8] J. Talonen, H. Hannien. Metall. Mater. Trans. A, **35**, 2401 (2004). DOI: 10.1007/s11661-006-0220-x
[9] B.A. Behrens, S. Hübner, A. Bouguecha, J. Knigge, K. Voges-Schwieger, K. Weilandt. Adv. Mat. Res., **137**, 1 (2010). DOI: 10.4028/www.scientific.net/AMR.137.1
[10] M. Smaga, F. Walther, D. Eifler. Mat. Sci. Eng. A, **483-484**, 394 (2008). DOI: 10.1016/j.msea.2006.09.140
[11] A.K. De, J.G. Speer, D.K. Matlock, D.C. Murdock, M.C. Mataya, R.J. Comstock. Metall. Mater. Trans. A, **37**, 1875 (2006). DOI: 10.1007/s11661-006-0130-y
[12] V.V. Mishakin, V.A. Klyushnikov, A.V. Gonchar. Tech. Phys., **60** (5), 665 (2015). DOI: 10.1134/S1063784215050163

[13] A. Rosen, R. Jago, T.J. Kjer. Mater. Sci., **7**, 870 (1972). DOI: 10.1007/BF00550434
[14] R. Dey, S. Tarafder, S. Sivaprasad. Int. J. Fatig., **90**, 148 (2016). DOI: 10.1016/j.ijfatigue.2016.04.030
[15] V.M.A. Silva, C.G. Camerini, J.M. Pardal, J.C.G. de Blás, G.R. Pereira. J. Mater. Res. Technol., **7**, 395 (2018). DOI: 10.1016/j.jmrt.2018.07.002
[16] S. Xie, L. Wu, Z. Tong, H.-En. Chen, Z. Chen, T. Uchimoto, T. Takagi. IEEE Trans. Magn. **54** (8), 1 (2018). DOI: 10.1109/TMAG.2018.2819123
[17] D. O'Sullivan, M. Cotterell, D.A. Tanner, I. Mészáros. NDT & E Int., **37**, 489 (2004). DOI: 10.1016/j.ndteint.2004.01.001
[18] S.H. Khan, F. Ali, A. Nusair Khan, M.A. Iqbal. Comp. Mater. Sci., **43** (4), 623 (2008). DOI: 10.1016/j.commatsci.2008.01.034
[19] C.S. Kim. Strength Mater., **50**, 41 (2018). DOI: 10.1007/s11223-018-9940-6
[20] A. Ould Amer, A.-L. Gloanec, S. Courtin, C. Touze. Proc. Eng., **66**, 651 (2013). DOI: 10.1016/j.proeng.2013.12.117
[21] V. Mishakin, A. Gonchar, K. Kurashkin, V. Klyushnikov, M. Kachanov. Int. J. Eng. Sci., **168**, 103567 (2021). DOI: 10.1016/j.ijengsci.2021.103567
[22] S. Xie, Z. Chen, H.-En. Chen, S. Sato, T. Uchimoto, T. Takagi,Y. Yoshida. Int. J. Appl. Electrom., **45**, 755 (2014). DOI: doi.org/10.3233/JAE-141903
[23] M.S. Ogneva, M.B. Rigmant, N.V. Kazantseva, D.I. Davydov, M.K. Korkh. Russ. J. Nondestruct., **53** (9), 644 (2017). DOI: 10.1134/S106183091709008X
[24] M.B. Rigmant, M.K. Korkh, D.I. Davydov, D.A. Shishkin, Yu.V. Korkh, A.P. Nichipuruk, N.V. Kazantseva. Rus. J. Nondestruct Testing, **51** (11), 680 (2015). DOI: 10.1134/S1061830915110030
[25] M. Bayerlein, H.J. Christ, H. Mughrabi. Mat. Sci. Eng. A, **114**, L11 (1989). DOI: 10.1016/0921-5093(89)90871-X
[26] H.J. Bassler, D. Eifler, M. Lang, G. Dobmann. *Characterization of the Fatigue Behavior of Austenitic Steel Using HTSL-SQUID. In Review of Progress in Quantitative Nondestructive Evaluation* (Springer, Boston 1998), DOI: 10.1007/978-1-4615-5339-7_207
[27] A.M. Sherman. Met. Trans. A, **6**, 1035(1975). DOI: https://doi.org/10.1007/BF02661357
[28] A. Glage, A. Weidner, T. Richter, P. Trubitz, H. Biermann. Europ. Sympos. on Martens.Transform., 05007 (2009). DOI: 10.1051/esomat/200905007
[29] S.K. Paul, N. Stanford, T. Hilditch. Int. J. Fatig., **106**, 185 (2018). DOI: 10.1016/j.ijfatigue.2017.10.005
[30] K.V. Kurashkin, V.V. Mishakin, S.V. Kirikov, A.V. Gonchar, V.A. Klyushnikov. Phys. Mesomech., **25**, 80 (2022). DOI: 10.1134/S102995992201009X
[31] V. Klyushnikov. Mat. Today: Proc., **19** (5), 2320 (2019). DOI: 10.1016/j.matpr.2019.07.679
[32] H. Biermann, M. Droste. *Austenitic TRIP/TWIP Steels and Steel-Zirconia Composites* (Springer, Cham. 2020), DOI: 10.1007/978-3-030-42603-3

Translated by A.Akhtyamov